ISSN 2394-3777 (Print)
ISSN 2394-3785 (Online)
Available online at www.ijartet.com
International Journal of Advanced Research Trends in Engineering and Technology (IJARTET)
Vol. 3, Special Issue 2, March 2016

Structural and Morphological behaviors of Ni incorporated MnO_2 nanocrystals

R. Poonguzhali[1], R. Gobi*[1], N. Shanmugam[1], G. Viruthagiri[1]
[1]Department of Physics, Annamalai University, Annamalai Nagar, Chidambaram 608 002, Tamilnadu, India.
Corresponding Author*E. Mail: alankoffi007@yahoo.co.in

Abstract

Pure MnO_2 and various levels of Ni doped MnO_2 nanocrystals have been synthesized by a chemical precipitation processes and characterized by various techniques. The X-ray diffraction patterns show the tetragonal structure of α-MnO_2.The FTIR spectrum confirms the presence of Mn-O bonds. Morphological studies show the synthesized particles to be combined nanospherical with nanorod structure.

Keywords: XRD, FT-IR,SEM,Nanoparticles.

1. Introduction

Selective synthesis of nanoscale materials with control-lable composition and morphology represents anincreasingly important research direction in nanosciences and nanotechnologies because the intrinsic properties of nanostructures are generally phase-, shape-, and sizedependent [1, 2]. Solution-chemical synthesis has been extensively employed as a versatile "bottom-up" synthetic methodology to synthesize inorganic nanostructures with diverse morphologies [3, 4]. In an aqueous system with surfactant, the organic and inorganic interfaces will determine the transporting behaviours of reactive species and thus affect the nucleation and growth of solid nanocrystals [5, 6].However, facile and simultaneous control over the oxidation state, crystal phase, and morphology of nanomaterials remains challenging because of elusive interactive thermodynamic and kinetic parameters. Fuel cells and metal/air batteries offer attractive alternatives to traditional fossil-fuel systems considering efficient and clean energy production, conversion, and storage [7, 8].Using oxygen in air as the cathode-active materials endows these systems with more profitable energy density and material efficiency.

Crystallized Manganese oxide (MnO_2) several crystalline structures, including α-, β-, γ-, and δ-MnO_2. Among them, α, β, γ and δ-MnO_2 have a tunnel structure (2 × 2 octahedral units for α-MnO_2, the relatively large tunnel structured phase; 1×1 octahedral units for β-MnO_2, the more compact and dense phase), and α-MnO_2 has a relatively open layered structure, It is well known that manganese oxides are considered as one of the cost-effective transition metal oxides for the next generation supercapacitors, due to their low cost, environmentally friendly nature, functional in neutral aqueous electrolytes and high theoretical specific capacitance.

In the present work, a simple chemical precipitation method has been reported for the preparation of Ni doped MnO_2Nanocrystals. Various molar percentages of nickel (0.025,0.05, 0.075,

ISSN 2394-3777 (Print)
ISSN 2394-3785 (Online)
Available online at www.ijartet.com
International Journal of Advanced Research Trends in Engineering and Technology (IJARTET)
Vol. 3, Special Issue 2, March 2016

0.1 and 0.125 M) were incorporated in MnO_2 and then characterized by a variety of techniques, including X-ray diffraction (XRD), Fourier transform spectroscopy (FTIR) and scanning electron microscope (SEM) with energy dispersive X-ray (EDX) analysis

2. Materials and Methods

2.1. Chemicals

All chemical reagents were purchased in refined grade (E. Merck) and used without further purification. All the solutions were prepared in deionized water. Manganese acetate tetra hydrate [$C_4H_6MnO_4.4H_2O$], nickel (III) nitrate nanohydrate [Ni $(NO_3)_3.9H_2O$] and potassium permanganate ($KMnO_4$) were used as precursors.

2.2. Synthesis of Pure and Ni ions doped MnO_2 nanocrystals

For the synthesis of Ni doped MnO_2, 6.12 g (0.5 M) of manganese acetate tetra hydrate [$C_4H_6MnO_4.4H_2O$] was dissolved in 30 ml of deionized water was stirred vigorously by magnetic stirrerand nickel(III) nitratenanohydrate [$Ni(NO_3)_3.9H_2O$] of preferred mole was (0.00, 0.025, 0.05, 0.075, 0.1 and 0.125 M) prepared in 20 ml aqueous were mixed drop by drop. Then, 5.92 g (1 M) of potassium permanganate in 50 ml of deionized water was added drop by drop to the above mixture. The entire mixture was stirred vigorously using a magnetic stirrer. After 5 hrs of stirring a dark brown coloured precipitate of precursor MnO_2 was obtained. The obtained precursor was washed alternately with deionized water and ethanol to remove the impurities. The washed products were dried in hot air oven at 80° C for 6 hrs to evaporate water and organic material to the maximum extent. Finally, the obtained product was annealed in a muffle furnace at 400° C for 3 hrs. The annealed powders were pulverized to fine powders using agate mortar for further characterizations. A similar method of preparation without the addition of Ni was used to synthesize undoped (Pure) MnO_2 nanocrystals.

2.3. Material characterization

The crystalline phase and particle size of pure and Ni doped MnO_2 nanoparticles were analyzed by X-ray diffraction (XRD) measurement which was carried out at room temperature by using X'PERT-PRO diffractometer system (scan step of 0.05° (2θ), counting time of 10.16 s per data point) equipped with a Cu tube for generating Cu K_α radiation (λ = 1.5406 Å); as an incident beam in the 2-theta mode over the range of 10°–80°, operated at 40 kV and 30 mA. The Fourier transform infrared (FTIR) spectra were carried out using SHIMADZU-8400 FTIR spectrometer in the range of 4000-400 cm^{-1}. The morphology of the product was observed by scanning electron microscopy (SEM; JEOL-JSM-56100) operating under 20 kV accelerating potential.

3. Results and discussion:

3.1 X- ray diffraction analysis

To determine the chemical composition and crystallite phase of the MnO_2 and Ni doped MnO_2 samples were examined by X-ray powder diffraction. The XRD pattern of MnO_2 and different concentration of Ni doped MnO_2 nanocrystals are shown inFig.1. The diffraction peaks at 12.50°, 25.02°, 36.5°, 37.8° and 66.9° correspond to the (110), (220), (400), (112) and (211) planes of

ISSN 2394-3777 (Print)
ISSN 2394-3785 (Online)
Available online at www.ijartet.com
International Journal of Advanced Research Trends in Engineering and Technology (IJARTET)
Vol. 3, Special Issue 2, March 2016

MnO_2. It is clearly seen that these peaks exhibit the tetragonal structure of α-MnO_2 nanocrystals as confirmed by the standard (JCPDS card No: 44-0141). The crystalline nature of the peak gradually increases with increasing Ni content [10]. The absence of any secondary peaks in the XRD pattern demonstrates the purity of the sample. The grain size was calculated using the Scherrer's formula and estimated as 9.8 nm for pure MnO_2. However the estimated sizes for different concentrations (0.025, 0.05, 0.075, 0.1 and 0.125 M) of Ni doped MnO_2 samples are 7.9, 5.0, 5.5, 7.5 and 9.0 nm, respectively. However, the characteristic peak of Ni can be obviously discerned in the XRD pattern in Fig.1revealing that not all of the doped Ni cations have been incorporated into the crystal lattice of α-MnO_2. Because of the ionic radius of Ni (0.72Å) is smaller than that of Mn (0.80Å), Ni can substitutefor Mn in octahedral site (CN=6) without a significant impact on the volume of the unit cell.

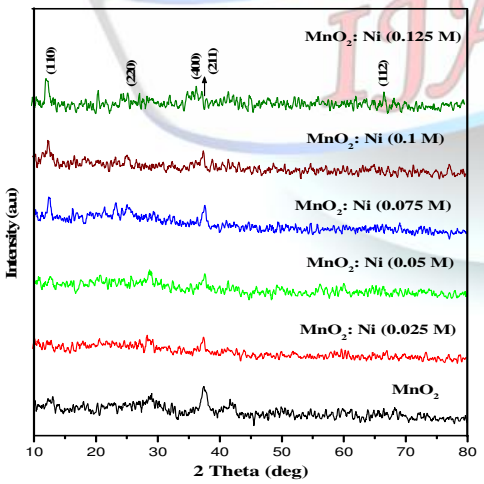

Fig. 1 X-ray diffraction patterns of pure and different levels of Ni doped MnO_2 nanocrystals

3.2 Functional group analysis

FTIR spectroscopy is an essential tool to study the presence of functional groups in the given sample. FTIR spectra of undoped and Ni doped MnO_2nanocrystals are shown in Fig.2. The absorptionbands at~3398 and ~1629 cm^{-1} encompass respectively to the O-H stretching and bending vibrations of absorbed water on the MnO_2 surface. All the samples show an absorption band at 2358 cm^{-1} which can be ascribed to the existence of CO_2 molecules in the air. The presence of absorption band at around 1382 cm^{-1} can be assigned to C-O stretching vibrations of acetate groups. FTIR measurements also confirm the existence of the large amount of hydroxyl groups on the surface of 0.125 M of Ni doped MnO_2, as learned from their much broaderabsorption band at 3398 cm^{-1} than that of other doped MnO_2 nanocrystals. The strongabsorption band between 522 and 493 cm^{-1} can be attributed to the stretching mode of Mn-O bond [11].

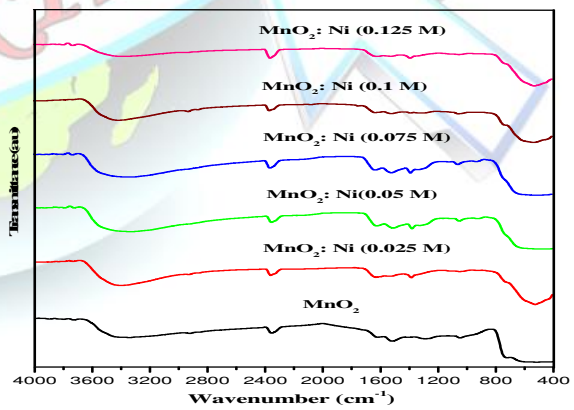

Fig. 2 FTIR spectra of pure and different levels of Ni doped MnO_2 nanocrystals

3.3 Morphological analysis

ISSN 2394-3777 (Print)
ISSN 2394-3785 (Online)
Available online at www.ijartet.com
International Journal of Advanced Research Trends in Engineering and Technology (IJARTET)
Vol. 3, Special Issue 2, March 2016

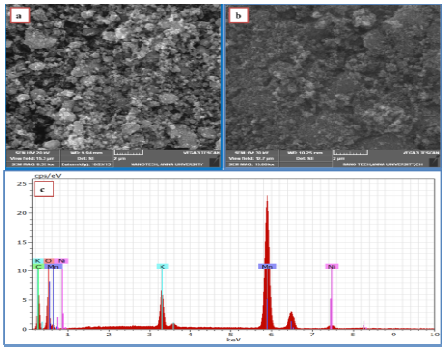

Fig. 3 (a, b) SEM image of pure and Ni (0.075 M) doped $MnO_2$and (c) corresponding EDX pattern

The SEM micrographs of MnO_2 and MnO_2: Ni (0.075 M) are presented in Fig.3(a, b). From the micrographs of undoped MnO_2, it is observed that most of the particles are spherical in shape with sizes in the range from 20-30 nm. However, the doped products are showing nanocrystals with spherical,triangular and rod like morphologies with sizes in the range of 15-20 nm. This indicates the effect of Ni doping on controlling the morphology of the MnO_2. The EDX spectrum of the doped MnO_2 is shown in Fig.3c, which confirms the presence of Mn, Ni, and O in the prepared samples.

4. Conclusion

Nanostructuredand poorly crystalline of manganese oxide and various levels of Ni doped manganese oxide were prepared by chemical precipitation method. It is clearly seen that these peaks exhibit the tetragonal structure of α-MnO_2 nanocrystals.The FTIR study confirms the presence of Mn-O bonds. The doped products are showing nanocrystals with spherical, triangular and rod like morphologies.Its suitable application in electrode material for supercapacitor.

Reference

[1] Q. Cheng, J. Tang, J. Ma, H. Zhang, N. Shinya, L.C. Qin, Carbon 49 (2011) 2917.

[2] Z.S. Wu, W. Ren, L. Xu, F. Li, H.M. Cheng, ACS Nano (2011) 5463.

[3] Z. Fan, J. Yan, T. Wei, L. Zhi, G. Ning, T. Li, F. Wei, Advanced Functional Materials 21 (2011) 2366.

[4] P.J. Hall, M. Mirzaeian, S.I. Fletcher, F.B. Sillars, A.J.R. Rennie, G.O. Shitta-Bey, G. Wilson, A. Cruden, R. Carter, Energy & Environmental Science 3 (2010) 1238.

[5] Sadayappan Nagamuthu, Subbukalai Vijayakumar, and Gopalan Muralidharan, Energy Fuels 27 (2013) 3508.

[6] A. Garcia-Gomez, P. Miles, T.A. Centeno, J.M. Rojo, Electrochem Solid State Letter 13 (2010) A112.

[7] Y.Y. Horng, Y.C. Lu, Y.K. Hsu, C.C. Chen, L.C. Chen, K.H. Chen, Journal of Power Sources 195 (2010) 4418.

[8] G.X. Hu, C.X. Li, H. Gong, Journal Power Sources 195 (2010) 6977.

ISSN 2394-3777 (Print)
ISSN 2394-3785 (Online)
Available online at www.ijartet.com
International Journal of Advanced Research Trends in Engineering and Technology (IJARTET)
Vol. 3, Special Issue 2, March 2016

[9] Y.R. Ahn, M.Y. Song, S.M. Jo, C.R. Park and D.Y. Kim, Nanotechnology 17(2006) 2865.

[10] N. Yu and L. Gao, ElectrochemCommun11 (2009)220.

[11] Songzhan Li, Jian Wen, Xiaoming Mo,Hao Long, Haoning Wang, JianboWang,
Guojia Fang, Journal of Power Sources 256 (2014) 206.